Applied Physics Letters

Transparent β-Si_3N_4 and γ-Si_3N_4 compacts synthesized with mixed-size precursor under high pressure and high temperature

Cite as: Appl. Phys. Lett. **119**, 171904 (2021); https://doi.org/10.1063/5.0070380
Submitted: 06 September 2021 • Accepted: 17 October 2021 • Published Online: 26 October 2021

Shuailing Ma, Yongsheng Zhao, Ruilian Tang, et al.

Applied Physics Letters ARTICLE scitation.org/journal/apl

Transparent β-Si_3N_4 and γ-Si_3N_4 compacts synthesized with mixed-size precursor under high pressure and high temperature

Cite as: Appl. Phys. Lett. **119**, 171904 (2021); doi: 10.1063/5.0070380
Submitted: 6 September 2021 · Accepted: 17 October 2021 ·
Published Online: 26 October 2021

Shuailing Ma,[1,2,3] Yongsheng Zhao,[1,3] Ruilian Tang,[1,4,a)] Bin Yang,[1] Qiang Tao,[2] Yan Li,[2] Jiaen Cheng,[2] Yu Wang,[5] Tian Cui,[2,6] and Pinwen Zhu[2,a)]

AFFILIATIONS

[1]Center for High Pressure Science & Technology Advanced Research, Beijing 100094, China
[2]Synergetic Extreme Condition High-Pressure Science Center, State Key Laboratory of Superhard Materials, College of Physics, Jilin University, Changchun 130012, China
[3]Deutsches Elektronen-Synchrotron DESY, Notkestrasse, 85, 22607 Hamburg, Germany
[4]School of Materials Science and Engineering, Changchun University of Science and Technology, Changchun 130022, China
[5]State Key Laboratory of Inorganic Synthesis and Preparative Chemistry, College of Chemistry, Jilin University, Changchun 130012, China
[6]Institute of High Pressure Physics, School of Physical Scientific and Technology, Ningbo University, Ningbo 315211, China

[a)]**Authors to whom correspondence should be addressed:** tangruilian626@cust.edu.cn and zhupw@jlu.edu.cn

ABSTRACT

Transparent polycrystalline ceramics exhibit improved mechanical and optical properties. However, synthesizing transparent ceramics without additives is nontrivial. Herein, we report the synthesis of two transparent ceramics (β-Si_3N_4 and γ-Si_3N_4) under high pressure and high temperature from a pure Si_3N_4 precursor with nano-/micro-dual grain sizes. Synthesized β-Si_3N_4 exhibited a significantly enhanced Vickers hardness reaching 24.2 GPa (at 10 N load) when transparency was achieved. Transparent nano-grained γ-Si_3N_4 exhibited a Vickers hardness of 37.3 GPa. These are the highest hardness values reported for these two phases at a 10 N load. Density and microstructure measurements suggest that the hardness and transparency of the specimens correlate with both the grain size and porosity/density. The negligible amount of pores accounts for the superior optical transparency and high hardness of two Si_3N_4 allotropes. As higher pressures can effectively suppress grain growth and minimize pores between grains, high-pressure sintering is demonstrated as an effective way to realize highly dense transparent ceramics.

The advantages of transparent ceramics include not only their optical merits but also their improved mechanical properties.[1–4] Owing to its high hardness and thermal stability, Si_3N_4 is used in cutting-tool inserts.[5] Although α-Si_3N_4 has a higher hardness than β-Si_3N_4, the latter is preferable for cutting tool applications because the stability of the former reduces at high temperatures.[6] At present, transparent ceramics can be obtained by a variety of procedures, including high-pressure sintering, spark plasma sintering (SPS), vacuum sintering, hot isostatic pressing sintering (HIP), and microwave sintering.[4,7–11] Transparent polycrystalline ceramics have been commercially used as optical lenses, laser amplifiers, optical windows, and so on.[10,12–15] However, additives are often used to increase transparency, which results in poor mechanical properties and limits their applications under harsh conditions.[7] Thus, it is critical to fabricate additive-free ceramics with superior mechanical and optical properties. High-pressure phase ceramics typically exhibit an exceptionally high hardness and are potential optical windows with good durability because of their superior mechanical properties. To date, transparent ceramic production is based mainly on ambient pressure phases, with a few exceptions, such as nano-polycrystalline diamond (NPD), stishovite, and coesite.[16,17] High-pressure phase ceramics generally cannot be sintered at ambient pressure using conventional methods. The development of rational synthesis procedures for functional high-pressure phase transparent ceramics appears to be highly promising but quite challenging.[18–21]

The low transmittance of ceramics produced by traditional techniques is mainly attributed to the presence of residual pores, large

grain size, and defective regions along grain boundaries.[3,22] On the basis on Mie scattering theory, Peelen and Metselaar calculated the effect of porosity on transmittance.[23] They speculated that the transmittance can reach its optical theoretical limit when there is a low pore content and small grain size less than 10 nm. In other words, the transmittance of the sintered ceramics can be improved by controlling the pore content and grain size. With regard to the Vickers hardness test, the indentations are generated by both elastic and plastic deformation under a rectangular pyramid diamond indenter.[24] For porous ceramic materials, an additional contribution to the indentation size is the porosity filling generated by the high stress beneath the indenter.[25] Several expressions for the relationship between hardness and porosity have been proposed. For example, Luo *et al.* proposed that the effect of porosity on hardness can be expressed by a negative exponential relationship, i.e., porosity is detrimental to hardness.[25] On the other hand, the hardness of ceramics is supposed to be greatly enhanced in the nano-crystalline regime, such as in the cases of NPD, nano-twinned diamond (NTD), nano-polycrystalline cubic boron nitride (NPBN), and nano-polycrystalline garnet.[1,16,26,27] Pore-free and nano-sized grains are common indicators of transparency and mechanical strength. Once pore-free and nano-sized grains are realized, hardness and optical transparency can be substantially enhanced at the same time. Extensive experimental and theoretical studies have been conducted on the reduction in pores and grain size in transparent engineering ceramics. Such transparent ceramics with pure nano-crystals are still difficult to realize because of the difficulty in removing inter-grain residual pores and suppressing grain growth. High-pressure sintering techniques can help to strengthen the inter-grain adhesion and suppress grain growth.[4,8,15,28,29] In addition, grains may deform plastically under high pressure (HP) to fit in the space available to them between adjacent grains.[30] Thus, it is expected that high-pressure synthesis promotes the formation of highly dense micrometer-grained and even nano-grained transparent ceramics. The feasibility of high-pressure sintering of traditional transparent ceramics has already been demonstrated for alumina, $MgAl_2O_4$, and YAG.[3,28–31]

In this context, we attempted to tailor the transmittance of Si_3N_4 by applying a high-pressure synthesis method and by mixing nano- and micro-sized precursor grains to obtain ceramics with a low concentration of pores and high hardness. We conducted a systematic synthesis of Si_3N_4 under a pressure range of 3.0–15.0 GPa and a temperature range of 1400–2000 °C. The optimized conditions yielded products of β-Si_3N_4 and γ-Si_3N_4 with transparency and/or hardness that have never been achieved before.

A sequence of synthesis trials at a fixed pressure of 5.5 GPa and different temperatures of 1400, 1600, 1800, and 2000 °C were conducted [Fig. 1(a)], along with those at a fixed temperature of 1800 °C and different pressures of 3.0, 3.5, 4.5, 5.5, and 15.0 GPa [Fig. 1(b)]. The recovered samples were examined by micro-focused x-ray diffraction (XRD). As shown in Fig. 1(a), the products synthesized at 1400 and 1600 °C remained in the starting phase. At higher temperatures (1800 and 2000 °C), all diffraction peaks from the specimens were identified as hexagonal β-Si_3N_4. Figure S1 shows the XRD patterns of the specimens synthesized at 5.5 GPa and 1800 °C with different sintering times, which suggests that the starting materials completely transformed into β-Si_3N_4 when the sintering time was longer than 5 min. Figure 1(b) presents the XRD patterns of the specimens synthesized at 1800 °C under different pressures. The starting material

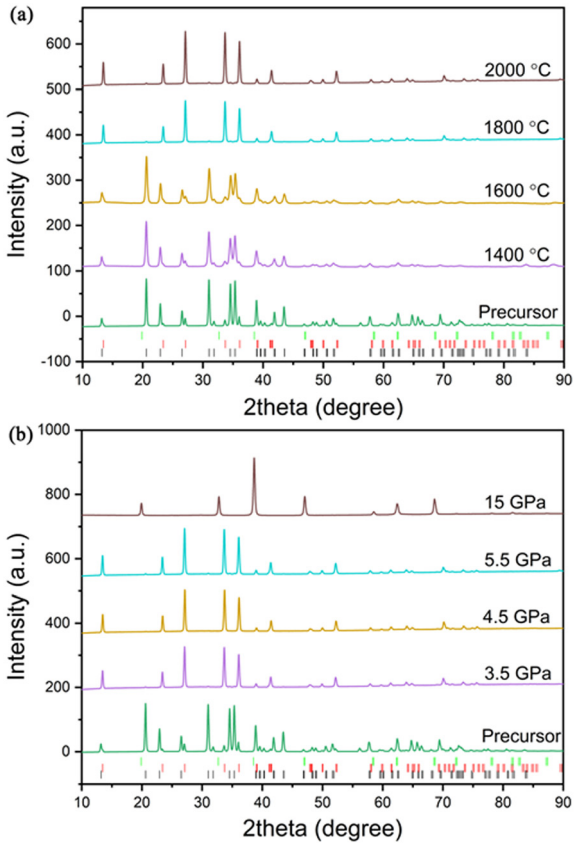

FIG. 1. (a) The x-ray diffraction patterns of Si_3N_4 specimens synthesized at 5.5 GPa and different temperatures as indicated. (b) The x-ray diffraction patterns of Si_3N_4 specimens synthesized at 1800 °C and different pressures as indicated. The expected diffraction peak positions are given at the bottom for α-Si_3N_4 (black), β-Si_3N_4 (red), and γ-Si_3N_4 (green) with space group $P3_1c$, $P6_3/m$, and $Fd\bar{3}m$, respectively.

transformed into β-Si_3N_4 at pressures of 3.5, 4.5, and 5.5 GPa. We also conducted a synthesis at 3.0 GPa, but the experiment ended with a blowout during heating, likely due to the decomposition of the Si_3N_4 precursor. At 15.0 GPa, the XRD results indicate that the sample transformed into cubic γ-Si_3N_4.

The typical optical appearances of the polished samples synthesized under different conditions are shown in Fig. 2. In our experiment, all the samples synthesized at a temperature of 1600 °C (bottom row) or lower were opaque, whereas those synthesized at 1800 °C (middle row) were transparent. When the synthesis temperature was increased to 2000 °C, the products (top row) become much less transparent. We performed a real in-line transmittance (RIT) of light measurement for samples recovered from different pressure conditions at 1800 °C, and the results are shown in Fig. S4. The RIT of visible light increased from 3.5 to 5.5 GPa, which suggests that the transparency of β-Si_3N_4 increases with the increasing synthesis pressure.

Figure 3(a) shows the microstructure of the starting material, which consists of mixed-size grains, dominated by large micro-grains of approximately 5–8 μm [Fig. 3(i)] and small nano-grains with a size

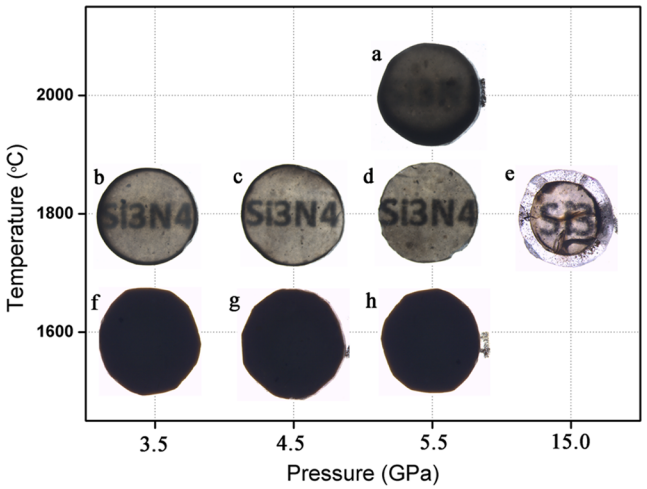

FIG. 2. Optical images of the polished samples synthesized at the pressure and temperature as indicated.

of approximately 100–200 nm. Nano-sized Si_3N_4 grains acted as a cement to bond the coarse micro-Si_3N_4 particles and occupy the porosity between micrograins. Therefore, highly dense and pore-free ceramics can be easily realized. The γ-Si_3N_4 sample synthesized at 15.0 GPa exhibited the highest transparency, according to the optical image results. The microstructures of the products obtained at 1400 and 1600 °C [Figs. 3(b) and 3(c)] are similar to those of the starting material [Fig. 3(a)]. They exhibited low compactness/high porosity, which may cause light dispersion and low transparency, although the sample formed at 1600 °C showed slightly better compactness than that at 1400 °C. When the synthesis temperature was increased to 1800 °C, the compacts exhibited a completely different, highly dense feature [Fig. 3(d)] with a grain size of approximately 1 μm [Fig. 3(i)]. The boundaries between different grains were less visible, and the pores were completely closed, which resulted in negligible light scattering and absorption at the grain boundaries. Although higher temperatures favor the elimination of pores, higher temperature causes significant grain growth and non-uniform crystallites, which are detrimental to optical transparency. This phenomenon was observed in the sample synthesized at 2000 °C [Figs. 2(a) and 3(e)]. Figures 3(d), 3(f), and 3(g) show the microstructures of the specimens synthesized at 1800 °C and pressures of 5.5, 4.5, and 3.5 GPa, respectively. Because HP restrains the grain growth during phase transition, grain size decreases with an increase in synthesis pressure [Fig. 3(i)]. In addition, HP is favorable for eliminating pores between neighboring grains. Consequently, specimens synthesized at higher pressures are composed of finer grains and a lower density of pores. The sample synthesized at 15.0 GPa transformed to γ-Si_3N_4 with a homogeneous grain size of approximately 120 nm, as shown in Fig. S6(b), with virtually no

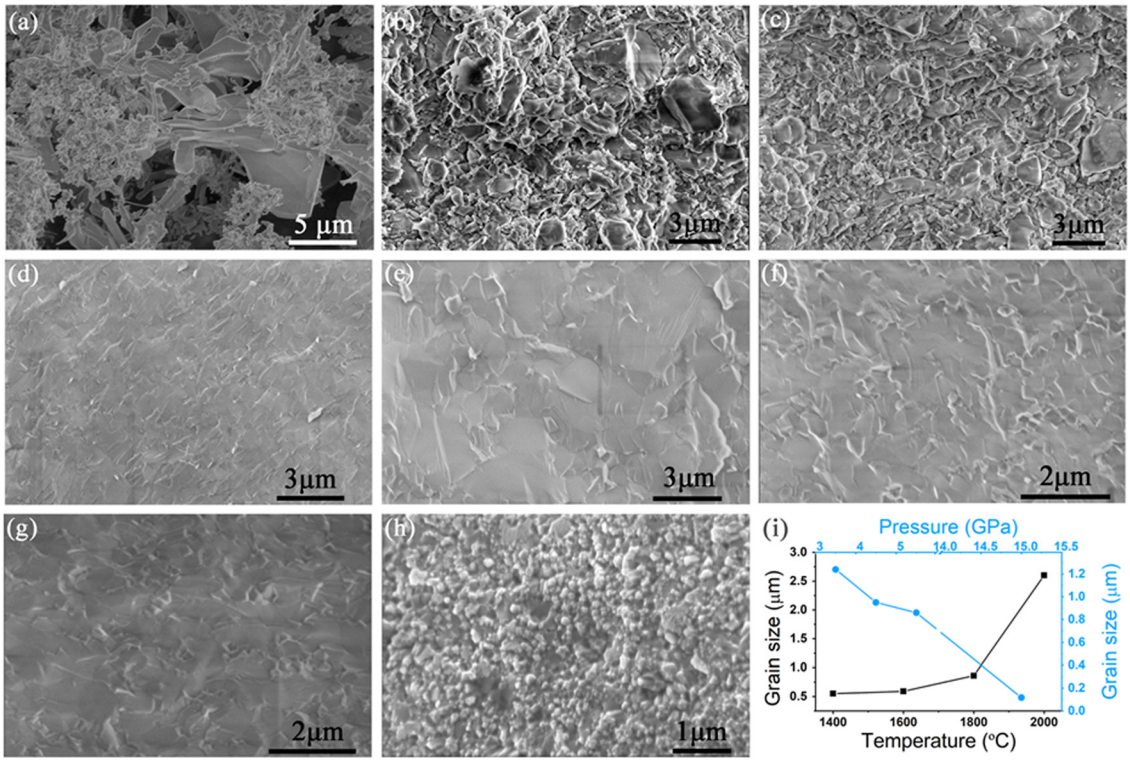

FIG. 3. The scanning electron microscope (SEM) images of (a) the starting materials; (b)–(e) the specimens synthesized at 5.5 GPa and temperatures of 1400, 1600, 1800, and 2000 °C, respectively; (f) and (g) the specimens synthesized at pressures of 4.5 and 3.5 GPa, respectively, and 1800 °C; and (h) the specimen synthesized at 15.0 GPa and 1800 °C. (i) Measured average grain sizes for corresponding specimens, plotted as a function of synthesis temperature at 5.5 GPa (black square symbols on primary scales) and a function of synthesis pressure at 1800 K (blue circular symbols on secondary scales).

pores or opening. A smaller grain size than the wavelength of visible light further promoted the transparency of samples.

The Vickers hardness of the polished products was measured using the indentation method as a function of the applied load up to 9.8 N (Fig. 4). The hardness of β-Si_3N_4 specimens increased with the increase in synthesis pressure [Fig. 4(a)]. At 5.5 GPa, the hardness of α-Si_3N_4 increased with sintering temperature (1400–1600 °C), which is in consistent with its microstructural features. When the sample just transforms to β-Si_3N_4 at 1800 °C, the sample hardness reaches its highest value of 19.3 GPa at 9.8 N loading. However, with a further increase in the synthesis temperature to 2000 °C, the hardness drops to 18.5 GPa (at 9.8 N loading) owing to notable grain growth [Fig. 3(i)]. A slight decrease in the sample density was also observed at this synthesis temperature (Table S1). The increase in porosity due to grain growth may be responsible for the decrease in hardness. To confirm the influence of grain growth, we varied the heating duration for 2, 5, 10, and 20 min during the syntheses at 5.5 GPa and 1800 °C. As shown in Fig. 4(c), the hardness declined when the heating time was either too short or too long, likely because of the imperfect crystallization or severe grain growth. With a 5 min heating duration, the product reached its highest hardness (24.2 GPa at 9.8 N load) because of the high relative density (RD, with regard to the ideal density from XRD) and small grain size. This Vickers hardness is the highest value achieved for β-Si_3N_4 at the same load, as shown in Table I.

Recently, Filgueira *et al.* (RD, 90%–97%)[36] and Hou *et al.* (RD, 97.2%)[32] reported a significant improvement in the hardness of β-Si_3N_4 transformed from α-Si_3N_4 through an high pressure and high temperature synthesis similar to that employed in this work. However, they used nearly uniform sizes of either micrometers (~2 μm) or nanometers (~200 nm), respectively, as their starting materials, whereas we started with a precursor with mixed grain precursor. The nano-grains serve as bonding agents between coarse micrometer particles during phase transition and minimize the porosity of the product. Remarkably, we were able to achieve transparency in polycrystalline β-Si_3N_4 and further improve the hardness by over 20%.

The hardness of transparent γ-Si_3N_4 specimen synthesized at 15.0 GPa was also measured (Fig. S7). The Vickers hardness was 39.7 (0.73) GPa at 4.9 N load and 37.3 (0.67) GPa at 9.8 N load. The highest Vickers hardness for γ-Si_3N_4 at 9.8 N reported so far is 34.9 (0.7) GPa by Norimasa *et al.*[2] Our specimen achieved a hardness of approximately 7% higher than this value, approaching the threshold for superhard materials (40 GPa). It even exceeds the well-known fourth-hardest material, SiO_2-stishovite, after diamond, BC_2N, and cubic boron nitride. Thus, γ-Si_3N_4 can be classified as the fourth hardest material.[16,17,44] Technically, the volume of sample will be drastically reduced with the increase in synthesis pressure. While high pressure gives high hardness γ-Si_3N_4 sample, low pressure fabrication gives relatively large β-Si_3N_4 specimens, which is also critical for application.

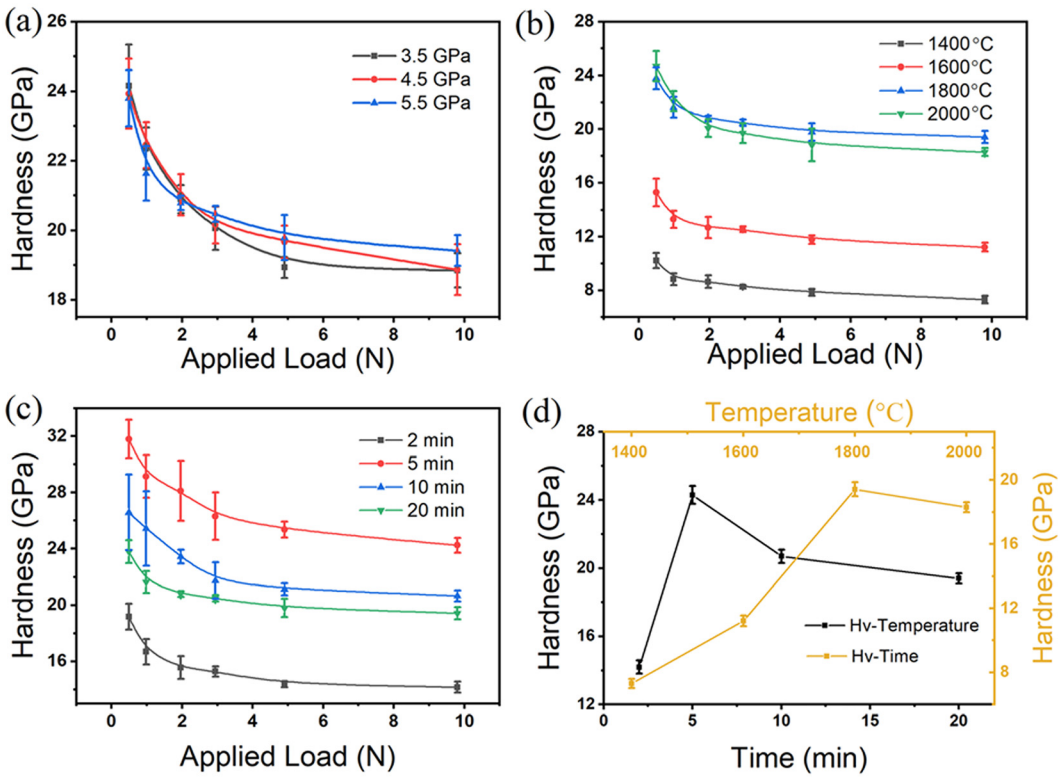

FIG. 4. The Vickers hardness of the Si_3N_4 specimens synthesized at (a) 1800 °C and different pressures; and (b) 5.5 GPa and different temperatures, as a function of the applied load. (c) The Vickers hardness of the β-Si_3N_4 specimens synthesized at 5.0 GPa and 1800 °C for 2 min (black), 5 min (red), 10 min (blue), and 20 min (green), as a function of the applied load. (d) The hardness (at 9.8 N load) variation of specimens sintered at 5.5 GPa with different synthesis temperatures and durations.

TABLE I. Summary of Vickers hardness and optical features of selected Si_3N_4 phases.

Reference	Phase	Hardness (GPa)	Load (N)	Optical feature
This study	β-Si_3N_4	24.2	9.8	Transparent
Hou *et al.*[32]	β-Si_3N_4	19.9	4.9	Opaque
Yu *et al.*[33]	β-Si_3N_4	18.5	4.9	[a]
Yu *et al.*[34]	β-Si_3N_4	16.1	4.9	[a]
Qadir *et al.*[35]	β-Si_3N_4	17.0	10	[a]
Filgueira *et al.*[36]	α-Si_3N_4 + β-Si_3N_4	21.3	9.8	[a]
Schneider *et al.*[37]	β-Si_3N_4	15.7	[a]	[a]
Nakamura *et al.*[38]	β-Si_3N_4	17	[a]	[a]
Teshima *et al.*[39]	β-Si_3N_4	15.7	98	[a]
Goto *et al.*[40]	β-Si_3N_4	15.7	[a]	[a]
This study	γ-Si_3N_4	37.3	9.8	Transparent
Nishiyama[2]	γ-Si_3N_4	34.9	9.8	Transparent
Wang *et al.*[41]	γ-Si_3N_4	31.0	9.8	Translucent
Tanaka *et al.*[50]	β-Si_3N_4	15.0	9.8	[a]
Tanaka *et al.*[51]	γ-Si_3N_4	43.0	0.01	[a]
Zerr *et al.*[42]	γ-Si_3N_4	30–43	5	[a]
Jiang *et al.*[43]	γ-Si_3N_4	35.31	[a]	Transparent

[a]Not reported.

From the RD point of view, micron-grained ceramics with lower RD normally exhibit low transparent or opaque features.[22] As listed in Table S1, the specimens synthesized at 3.5, 4.5, and 5.5 GPa present an RD of 97.9 (0.3)%, 98.4 (0.5)%, and 98.6 (0.3)%, respectively. These RD qualities agree closely with our microstructure measurements. The β-Si_3N_4 specimen with the highest RD and small grain size possessed the highest optical transparency and hardness, indicating that high density and small grain size favor the hardness as they do transmittance.

Two transparent Si_3N_4 products (β-Si_3N_4 synthesized at 5.5 GPa and 1800 °C and γ-Si_3N_4 synthesized at 15.0 GPa and 1800 °C) were investigated using transmission electron microscopy (TEM). Figure 5(a) shows a high-resolution TEM (HRTEM) image of β-Si_3N_4. The grain junctions between two grains are within 1 nm, which explains its high RD and high optical transparency of β-Si_3N_4. Figure 5(b) shows a bright-field TEM image of γ-Si_3N_4. The sample presented a homogenously granular texture with a grain size of approximately 100–200 nm, in agreement with the SEM results. The HRTEM images of the multigrain junctions of γ-Si_3N_4 [Figs. 5(c) and 5(d)] demonstrate that the thickness of intergranular films (IGFs) was quite thin. It was difficult to observe any defective regions in γ-Si_3N_4. Apart from the equilibrium upon crystallization of the new phase, ultra-HP initiates the deformation of grains and accelerates the yielding of "Y"-shaped grain junctions. The emergence of "Y" triple junctions indicates that individual grains crystallize up to the grain boundary and grains are closely interlocked. The similar morphologies of the two high-transparency specimens confirm that transparent compacts usually exhibit a low density of pores and defect-free boundaries. Ultra-HP facilitates the formation of such highly dense and crystalline microstructures.

Previously reported NPD synthesized from graphite by Irifune *et al.* consisted of minute (10–20 nm) crystals and larger elongated

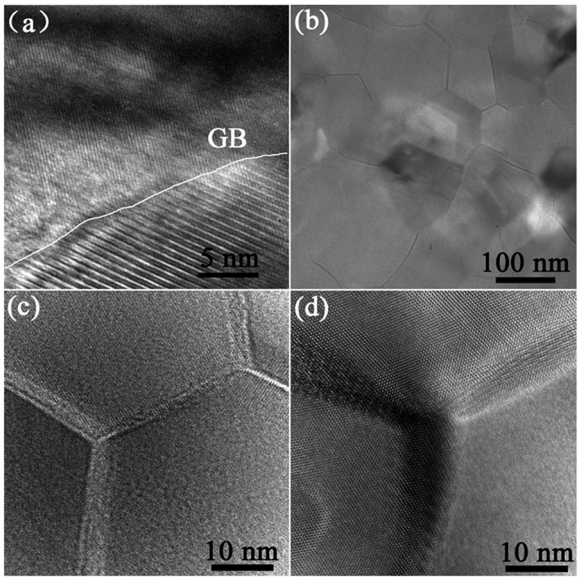

FIG. 5. (a) High-resolution transmission electron microscopy images of β-Si_3N_4 specimen synthesized at 5.5 GPa. (b) Bright-field TEM image. (c) and (d) HRTEM images of γ-Si_3N_4 synthesized at 15.0 GPa.

(100–200 nm) crystals.[16] Their subsequent study[45] indicates that the starting materials consist of large graphite crystallites up to 1 μm and small crystallites below 100 nm. The minute crystals originate from the small graphite grains through a diffusion-controlled process, and the elongated diamond crystals are transformed from the large graphite crystallites by the martensitic transformation mechanism.[45] However, in our experiment, the mixed micro- and nano-sized precursors transformed into a homogenously granular microstructure of γ-Si_3N_4 at 15.0 GPa. This result suggests that the transformation mechanism from α-Si_3N_4 to γ-Si_3N_4 is different from that from graphite to NPD, that is, diffusion-controlled nucleation and growth. Although α-Si_3N_4 and β-Si_3N_4 have similar layered structures, the transformation from α-Si_3N_4 to β-Si_3N_4 is reconstructive, requiring short-range diffusion.[46,47] Previous theoretical and experimental studies[48,49] demonstrated that pressure (P) influences diffusion-controlled nucleation through the nucleation activation energy, ΔG^*,

$$\left(\frac{\partial(\Delta G^*)}{\partial P}\right) = -\frac{32\pi\sigma^3}{3}\frac{\Delta V}{(\Delta G)^3},$$

where σ is the interfacial energy, which is not sensitive to pressure; $\Delta V = V_\alpha - V_\beta$ is the molar volume between the starting phase (α) and ending phase (β); and $\Delta G = G_\alpha - G_\beta$ is the free energy difference between the α and β phases. In both of $\alpha-\beta$ and $\alpha-\gamma$ phase transformations, $\Delta V > 0$, that is, $\partial(\Delta G^*)/\partial P < 0$, indicating that HP decreases the nucleation activation energy and critical nuclei size of the higher pressure phases.[48] In other word, pressure promotes the nucleation in α–β and α–γ phase transformations. This result explains why smaller grain size is achieved at higher pressures in these syntheses.

The direct conversion method at HP produced pore-free micrometer-grained β-Si_3N_4 and nano-grained γ-Si_3N_4 ceramics with mixed-size starting materials. Compared to previously published results,

nano-/micro-dual grain sizes of the starting materials in our study play a critical role in forming highly dense polycrystalline Si_3N_4 allotropes that present both improved hardness and optical transparency. The optical transparency of Si_3N_4 ceramics is sensitive to the pores and defects at the grain boundaries. Optimized experimental conditions help to achieve such results through the copious nucleation promoted by HP and restrained growth at the lowest possible temperature and short synthesis time. High-pressure synthesis has been demonstrated to be a powerful tool for realizing highly dense micro- and nano-polycrystalline ceramics with excellent mechanical and optical properties.

See the supplementary material for the experimental details and additional data.

This work was supported by the National Natural Science Foundation of China (under Grant Nos. 11904119 and 11974131), National Key R&D Program of China (2018YFA0703400), and the Youth science foundation of Changchun University of Science and Technology (Grant No. XQNJJ-2018-15).

AUTHOR DECLARATIONS

Conflict of Interest

The authors have no conflicts to disclose.

DATA AVAILABILITY

The data that support the findings of this study are available from the corresponding authors upon reasonable request.

REFERENCES

[1]T. Irifune, K. Kawakami, T. Arimoto, H. Ohfuji, T. Kunimoto *et al.*, Nat. Commun. **7**, 13753 (2016).
[2]N. Nishiyama, R. Ishikawa, H. Ohfuji, H. Marquardt, A. Kurnosov *et al.*, Sci. Rep. **7**, 44755 (2017).
[3]T. C. Lu, X. H. Chang, J. Q. Qi, X. J. Luo, and Q. M. Wei, Appl. Phys. Lett. **88**, 213120 (2006).
[4]F. M. Liu, D. W. He, Q. Wang, W. Ding, J. Liu *et al.*, Scr. Mater. **122**, 54–58 (2016).
[5]D. W. Freitag and D. W. Richerson, *Opportunities for Advanced Ceramics to Meet the Needs of the Industries of the Future*, 1st ed. (Office of Industrial Technologies, 1998), p. 2.
[6]L. L. Wang, T. Y. Tien, and I. W. Chen, J. Am. Ceram. Soc. **86**, 1578 (2003).
[7]B. N. Kim, K. Hiraga, K. Morita, and H. Yoshida, Scr. Mater. **57**, 607–610 (2007).
[8]S. Grasso, H. Yoshida, H. Porwal, Y. Sakka, and M. Reece, Ceram. Int. **39**, 3243–3248 (2013).
[9]K. Hayashi, O. Kobayashi, S. Toyoda, and K. Morinaga, Mater. Trans. JIM **32**, 1024–1029 (1991).
[10]J. P. Cheng, D. Agrawal, Y. J. Zhang, and R. Roy, Mater. Lett. **56**, 587–592 (2002).
[11]X. J. Mao, S. W. Wang, S. Shimai, and J. K. Guo, J. Am. Ceram. Soc. **91**, 3431–3433 (2008).
[12]R. Pązik, P. Głuchowski, D. Hreniak, W. Stręk, M. Roś *et al.*, Opt. Mater. **30**, 714–718 (2008).
[13]N. Tan, Z. L. Kou, Y. H. Ding, Y. Leng, C. J. Liu *et al.*, Scr. Mater. **65**, 819–822 (2011).
[14]K. Liu, D. W. He, H. M. Wang, T. C. Lu, F. Li *et al.*, Scr. Mater. **66**, 319–322 (2012).
[15]R. P. Yavetskiy, E. A. Vovk, A. G. Doroshenko, M. I. Danylenko, A. V. Lopin *et al.*, Ceram. Int. **37**, 2477–2484 (2011).
[16]T. Irifune, A. Kurio, S. Sakamoto, T. Inoue, and H. Sumiya, Nature **421**, 599–600 (2003).
[17]N. Nishiyama, S. Seike, T. Hamaguchi, T. Irifune, M. Matsushita *et al.*, Scr. Mater. **67**, 955–958 (2012).
[18]P. Mohanty, Y. W. Fei, and K. Landskron, J. Am. Chem. Soc. **131**, 9638–9639 (2009).
[19]P. Mohanty, V. Ortalan, N. D. Browning, I. Arslan, and Y. W. Fei, Angew. Chem. Int. Ed. **49**, 4301–4305 (2010).
[20]V. Stagno, M. Mandal, K. Landskron, and Y. W. Fei, Phys. Chem. Miner. **42**, 509–515 (2015).
[21]S. Najiba, S. J. Juhl, M. Mandal, C. Liu, A. Durygin *et al.*, Scr. Mater. **162**, 350–354 (2019).
[22]R. Apetz and M. P. B. v Bruggen, J. Am. Ceram. Soc. **86**, 480–486 (2003).
[23]J. G. J. Peelen and R. Metselaar, J. Appl. Phys. **45**, 216 (1974).
[24]X. Q. Chen, H. Y. Niu, D. Z. Li, and Y. Y. Li, Intermetallics **19**, 1275–1281 (2011).
[25]J. Luo and R. Stevens, Ceram. Int. **25**, 281–286 (1999).
[26]Q. Huang, D. L. Yu, B. Xu, W. T. Hu, Y. M. Ma *et al.*, Nature **510**, 250–253 (2014).
[27]M. X. Zhao, Z. L. Kou, Y. J. Zhang, B. Peng, Y. P. Wang *et al.*, Appl. Phys. Lett. **118**, 151901 (2021).
[28]J. A. Wollmershauser, B. N. Feigelson, S. B. Qadri, G. R. Villalobos, and M. Hunt, Scr. Mater. **69**, 334–337 (2013).
[29]N. Nishiyama, T. Taniguchi, H. Ohfuji, K. Yoshida, F. Wakai *et al.*, Scr. Mater. **69**, 362–365 (2013).
[30]F. M. Liu, D. W. He, P. P. Liu, H. K. Wang, C. Xu *et al.*, J. Appl. Phys. **114**, 233504 (2013).
[31]R. Fedyk, D. Hreniak, W. Łojkowski, W. Stręk, H. Matysiak *et al.*, Opt. Mater. **29**, 1252–1257 (2007).
[32]Z. Q. Hou, H. K. Wang, Y. N. Yang, X. D. Song, S. P. Chen *et al.*, Ceram. Int. **46**, 12449–12457 (2020).
[33]J. J. Yu, S. K. Sun, W. X. Wei, W. M. Guo, K. Plucknett *et al.*, Ceram. Int. **45**, 16703–16706 (2019).
[34]J. J. Yu, W. M. Guo, W. X. Wei, H. T. Lin, and C. Y. Wang, J. Eur. Ceram. Soc. **38**, 3457–3462 (2018).
[35]A. Qadir, Z. Fogarassy, Z. E. Horváth, K. Balazsi, and C. Balazsi, Ceram. Int. **44**, 14601–14609 (2018).
[36]M. Filgueira, Á. L. N. Nascimento, M. P. Oliveira, D. Souza, and Z. A. S. Guimarães, J. Braz. Soc. Mech. Sci. Eng. **40**, 118 (2018).
[37]J. Schneider, P. Miranzo, M. I. Osendi, and M. Belmonte, J. Am. Ceram. Soc. **99**, 241–248 (2016).
[38]M. Nakamura, K. Hirao, Y. Yamauchi, and S. Kanzaki, J. Am. Ceram. Soc. **84**, 2579–2584 (2001).
[39]H. Teshima, K. Hirao, M. Toriyama, and S. Kanzaki, J. Ceram. Soc. Jpn. **107**, 1216–1220 (1999).
[40]Y. Goto, H. Ohta, and M. Komatsu, J. Ceram. Soc. Jpn. **94**, 167–171 (1986); available at https://pascal-francis.inist.fr/vibad/index.php?action=getRecordDetail&idt=8712213.
[41]W. D. Wang, D. W. He, M. J. Tang, F. J. Li, L. Liu *et al.*, Diamond Relat. Mater. **27–28**, 49–53 (2012).
[42]A. Zerr, M. Kempf, M. Schwarz, E. Kroke, M. Göken *et al.*, J. Am. Ceram. Soc. **85**, 86–90 (2002).
[43]J. Z. Jiang, F. Kragh, D. J. Frost, K. Ståhl, and H. Lindelov, J. Phys.: Condens. Matter **13**, L515–L520 (2001).
[44]H. Sumiya, Y. Ishida, K. Arimoto, and K. Harano, Diamond Relat. Mater. **48**, 47–51 (2014).
[45]H. Ohfuji, S. Okimoto, T. Kunimoto, F. Isobe, H. Sumiya *et al.*, Phys. Chem. Miner. **39**, 543–552 (2012).
[46]H. Suematsu, M. Mitomo, T. E. Mitchell, J. J. Petrovic, O. Fukunaga *et al.*, J. Am. Ceram. Soc. **80**, 615–620 (1997).
[47]V. K. Sarin, Mater. Sci. Eng. A **105–106**, 151–159 (1988).
[48]D. Turnbull and J. C. Fisher, J. Chem. Phys. **17**, 71 (1949).
[49]W. H. Wang, T. Okada, P. Wen, X. L. Wang, and M. X. Pan, Phys. Rev. B **68**, 184105 (2003).
[50]I. Tanaka, G. Pezzotti, T. Okamoto, *et al.*, J. Am. Ceram. Soc. **72**, 1656 (1989).
[51]I. Tanaka, F. Oba, T. Sekine, *et al.*, J. Mater. Res. **17**, 731 (2002).